Sensorless Vector Control of Three Phase Induction Motor Based on Full Neural Estimator and Controller

Fatma H. Faris*

Received on: 18/1/2011
Accepted on: 5/5/2011

Abstract

Conventional vector control of A.C drives are widely used in industry and many other applications, where high dynamic performance is required, this type of controller usually needs costly speed sensor. Sensorless vector control is strongly recommended in the dangerous sites and hostile environment, also to reduce cost and increase reliability. In this way the rotor speed can be estimated from the terminal voltage and current by means of DSP microprocessor. The DSP-estimator is very complex hardware, has many operation problems, and very sensitive to the electromagnetic interference (EMI). This paper proposes using the Artificial Neural Network (ANN) to estimate the rotor speed, flux vector, torque, and unit vectors instead of DSP-estimator. Also, the neural-based controller is proposed too. The ordinary vector control with speed sensor and sensorless vector control based on DSP-estimator PI-controller are represented in this work as point of comparison. Also, the mathematical representation and simulation of the three phase induction motor is illustrated in this paper. The proposed method, neural-based sensorless vector controller and estimator, gives superior performance in different speed with respect to DSP-estimator PI-controller.

Keywords: Sensorless Vector Control, Neural Estimation, PI Neural-Based Controller.

مسيطر المتجه بدون متحسس السرعة للمحرك الحثي الثلاثي الطور المستند على أستخدام عصبي كامل في المخمن والمسيطر

الخلاصة

مسيطر المتجه التقليدي لسواقات التيار المتناوب واسع الأستخدام في الصناعة وعدة تطبيقات أخرى حيث تتطلَّب أداءاً ديناميكياً عالياً، ويحتاج هذا النوع من المسيطرات عادةً الى متحسس سرع مكلف. في المواقع الخطرة والبيئه العدائيه يوصى بقوة أستخدام مسيطر المتجه بدون متحسس سرعه وأيضا لتخفيف الكلفه وزيادة الموثوقيه. لهذه الأغراض يمكن تخمين سرعة الدوار من تيار وجهد بواسطة معالج دقيق. أن التخمين بواسطة المعالج الدقيق معقد جداً وذو مشاكل عملية عديدة، كما أنه حساس جداً للتداخلات الكهرومغناطيسية. يقترح هذا البحث أستخدام الشبكة العصبية الإصطناعية لتخمين سرعة الدوار ومتجه المجال والعزم ومتجهات الوحدة بدلاً عن المعالج الدقيق. كما ويقترح هذا البحث أستخدام المسيطر العصبي أيضاً. مسيطر المتجه التقليدي بأستخدام متحسس سرعة وبدون متحسس سرعة قُدّمَ في هذا العمل للمقارنة. كما وقُدّمَ التمثيل الرياضي والمحاكاة للمحرك الحثي الثلاثي الطور في هذه الورقة. أعطت الطريقه المقترحه لمسيطر المتجه بدون متحسس سرعة والمستند على أساس عصبي للمسيطر والمخمن أداءاً رائعاً لسرع مختلفه مقارنةً مع طريقة المسيطر والمخمن بأستخدام المعالج الدقيق.

***Electrical and Electronic Engineering Department, University of Technology/Baghdad**

1. Introduction

Modern microelectronics has changed the world of electrical drives, where AC machines seem to have completely conquered the field of speed variable drives. Today's modern microcontrollers and Digital Signal Processors DSP make the implementation of the necessary complicated control structures possible and the high demand performance can be achieved [1].

The most popular speed control method of the induction motor is the open loop Variable Voltage Variable Frequency (VVVF), because of its simplicity, and these types of motors are widely used in industrial applications. Traditionally, the Volt/Hz is controlled by means of D.C-A.C pulse width modulation inverter in order to maintain the air-gap flux approximately at its rated value, this type of control called "scalar control". Unfortunately, the inherent coupling effect for both torque and flux are functions of voltage or current and frequency (i.e. during Volt/Hz variation both torque and flux be varied too), which gives sluggish response and the system is easily prone to instability because of high order system effect [1, 2].

This problem can be solved by vector control, which invented at 1970s, and the demonstration that; an induction motor can be controlled likes a separately excited D.C. motor, brought a renaissance in the high performance control of A.C. drives, vector control is also known as decoupling, orthogonal, or trans-vector control. The principle of this method is to rotate the direct axis always in the same direction of the rotor pole axis, or by aligned the rotor flux vector $\overline{\psi}_r$ on the d-axis. This can be done by estimating the exact unit vector ($\cos\theta_e$ and $\sin\theta_e$). In this way it's essential to estimate the flux vector $\overline{\psi}_r$

And the unit vector by using complex digital signal processing (DSP) and microcomputer analysis[1, 2].

Ongoing research has concentrated on the elimination of the speed sensor at the machine shaft without deteriorating the dynamic performance of the drive control. In this way the rotor speed can be estimated too from the measuring of stator current and voltage instead of using speed encoder or sensor, which reduce the cost and operation problems [1, 3].

Nowadays, the Artificial Intelligent System (AIS) has penetrated deeply into electrical engineering field and their applications in power electronics and motion control appears very promising [1, 4]. The artificial neural system is one of the most powerful intelligent systems with improved design and performance features.

The sensorless vector control of 3-phase induction motor by using DSP estimation and PI controller is illustrated in this paper. Also, this paper proposed the artificial neural networks in estimating the flux vector $\overline{\psi}_r$, the unit vector ($\cos\theta_e$ and $\sin\theta_e$), the electromagnetic torque T_e, and rotor speed ω_r instead of using the complex microprocessor DSP analysis.

The outlines of this paper can be divided into three main steps:

i- Demonstrate the ordinary DSP estimator vector control with speed sensor feedback signal.

ii- Demonstrate the sensorless DSP estimator vector control.

iii- Demonstrate the sensorless neural network estimator vector control.

2. Topics for Review

Before entering deeply in vector control, some principles of A.C. drives and system stages must be briefly reviewed to understand system

operation. The overall system is consisting of three main stages as shown in figure (1):

i- Voltage-fed Sinusoidal Pulse Width Modulation (SPWM) inverter.
ii- Three phase induction motor model.
iii- Controller and estimator.

The last one will be discussed in details later.

2.1 Volt/Hz Control

The characteristics of 3-phase induction motor have different forms as the variation of input voltage and frequency. The operation characteristics can be divided into three regions [1, 5]:

i- Constant torque region; where the volt/Hz is kept constant to maintain flux and pull-out torque at their maximum limits.
ii- Constant power region 1; where the stator voltage reaches rated value and the frequency increased beyond synchronous frequency. The air-gap flux decreases but the stator current maintained constant by increasing the slip.
iii- Constant power region 2; where the torque is inversely proportion with square of speed, because of both of current and flux reduce with speed increasing.

The last two regions are known as field weakening region [1, 2].

2.2 Sinusoidal PWM Voltage-Fed Inverter

The pulse width modulation techniques have wide simple and complex types, the Sinusoidal Pulse Width Modulation (SPWM) is the most popular used method of A.C. drives, but it's not the efficient method [1, 6]. Voltage source inverter (VSI) should have a stiff source at the input [1], that is, its Thevenin impedance ideally is zero. Thus, a large capacitor can be connected at the input if the voltage source is not stiff. A practical (VSI) consist of power bridge devices with three output legs, each consist of two power switches and two freewheeling diodes, the inverter is supplied from D.C. voltage source via LC or C filter. In sinusoidal PWM the three output legs considered as three independent push-pull amplifiers [6]. The gating signals of each push-pull stage generated by comparing a constant level triangle signal of frequency (f_c) called "carrier signal", with 3-phase sinusoidal signals of frequency (f_r) called "reference signals", which has variable amplitude to get the desired output voltage, this comparison leads to generate a sequence of variable width pulses used to gating each switch in the push-pull stage.

The output phase voltage:

V_{ao} = is the output phase voltage measured to the center of the input D.C. voltage.

V_{an} = is the output phase voltage measured to isolated neutral of three-phase load such as induction motor.

Where:

$$\begin{bmatrix} V_{an} \\ V_{bn} \\ V_{cn} \end{bmatrix} = \frac{1}{3}\begin{bmatrix} 2 & -1 & -1 \\ -1 & 2 & -1 \\ -1 & -1 & 2 \end{bmatrix} \begin{bmatrix} V_{ao} \\ V_{bo} \\ V_{co} \end{bmatrix} \quad \ldots\ldots (1)$$

$V_{ao} = 0.5mV_d \sin(\omega t)$+high-frequency (M $\omega_c \pm N\omega$) [1] …… (2)

Where: ω = fundamental frequency; ω_c=carrier frequency; M and N are integers and M+N =odd, m=modulation index is defined as [1, 6]:

$$m = \frac{V_P}{V_T} \quad \ldots\ldots\ldots\ldots (3)$$

Where: V_P = peak of modulating signal, V_T = peak of triangle signal. At m= 1, the maximum value of fundamental peak = $0.5V_d$ which is 78.54% of the peak fundamental voltage of the square-wave ($2V_d/\pi$) which called the linear modulation region. To further increase the amplitude of the output voltage, the amplitude of the modulating signals

exceeds the amplitude of the carrier signal which leads to enter into quasi-PWM region called "over modulating region" causing increase in the low order harmonics. Further increasing modulation index tends to obtain square wave at maximum possible output fundamental ($2V_d/\pi$) [1, 6].

By using MATLAB/SIMULINK PROGRAM, the SPWM inverter can be simulated, firstly generation of the carrier triangle signal and the three modulating signals by using internal timer and the rated frequency (50 H_Z) to obtain the angular speed ($\omega_e t$), then multiplying the angular speed and the amplitude of the signal by the frequency command (f^*_{com}) and voltage command (V^*_{com}) respectively. Secondly, compared the two signal sets to generate the switching signals of three switches used as three push-pull devices. The output of the switches gives (V_{ao}, V_{bo}, V_{co}) then the three phase to load neutral (V_{an}, V_{bn}, V_{cn}) can be achieved by implementing equation (1). Figure (2) illustrated the complete simulation of SPWM inverter, and the output phase voltage can be shown in figure (3).

2.3 Modeling and Simulation of Three Phase I.M.

The mathematical representation of an induction motor can be looked on as transformer with moving secondary winding, where the coupling coefficients between the stator and rotor phases change continuously with the change of rotor position [1, 6]. The machine model can be described by differential equation with time varying mutual inductances, but such model tends to be very complex. Therefore, axis transformation is applied to transfer the three phase parameters (voltage, current and flux) to two–axis frame called (dq-axis stationary frame or park transformation). Park transformation is applied to refer the stator variables to a synchronously rotating reference frame fixed in the rotor, by such transformation the stator and rotor parameters rotate in synchronous speed and all simulated variables in the stationary frame appear as d.c. quantities in the synchronously rotating reference frame [1, 6].

The per-phase equivalent circuit diagrams of an I.M. in two- axis synchronously rotating reference frame are illustrated in figure (4). From the circuit diagram the following equations can be written [1]:

- Stator equation:

$$V_{qs}^{\ e} = R_s i_{qs}^{\ e} + \frac{d\Psi_{qs}}{dt} + w_e \Psi_{ds} \quad \text{.....(4)}$$

$$V_{ds}^{\ e} = R_s i_{ds}^{\ e} + \frac{d\Psi_{ds}}{dt} - w_e \Psi_{qs} \quad \text{.....(5)}$$

- Rotor equation:

$$V_{qr}^{\ e} = R_r i_{qr}^{\ e} + \frac{d\Psi_{qr}}{dt} + (w_e - w_r)\Psi_{dr} \quad \text{...(6)}$$

$$V_{dr}^{\ e} = R_r i_{dr}^{\ e} + \frac{d\Psi_{dr}}{dt} - (w_e - w_r)\Psi_{qr} \quad \text{...(7)}$$

Where: the superscript notation "*e*" referred to the synchronously rotating reference frame quantities.

It's obviously that in squirrel cage I.M V_{qdr}=0, then the pervious equation can be rewritten:

$$\frac{d\Psi_{qs}}{dt} = V_{qs}^{\ e} - R_s i_{qs}^{\ e} - w_e \Psi_{ds} \quad \text{....(8)}$$

$$\frac{d\Psi_{ds}^{\ e}}{dt} = V_{ds}^{\ e} - R_s i_{ds}^{\ e} + w_e \Psi_{qs} \quad \text{....(9)}$$

$$\frac{d\Psi_{qr}}{dt} = -R_r i_{qr}^{\ e} - (w_e - w_r)\Psi_{dr} \quad \text{....(10)}$$

$$\frac{d\Psi_{dr}}{dt} = -R_r i_{dr}^{\ e} + (w_e - w_r)\Psi_{qr} \quad \text{....(11)}$$

The development torque by interaction of air gap flux and rotor current can be found as:

$T_e=(3/2)(P/2)\overline{\Psi_m} X \overline{I_r}$ .....(12)

By resolving the variables into d^e-q^e components:

$T_e=(3/2)(P/2)(\Psi_{ds} i_{qs}^{\ e} - \Psi_{qs} i_{ds}^{\ e})$ ..(13)

The dynamic torque equation of the rotor:

$$T_e = T_L + (\frac{2}{P}) J \frac{dw_r}{dt} \quad .....(14)$$

Where: ω_r = is the rotor speed; P: no. of poles; J= rotor inertia; T_L= load torque.

$$i_{ds}^{\ e} = \frac{\Psi_{ds} - \Psi_{qm}}{L_s} \quad .....(15)$$

The stator current can be found by:

$$i_{qs}^{\ e} = \frac{\Psi_{qs} - \Psi_{dm}}{L_s} \quad .....(16)$$

The air gap flux:

$$\Psi_{qm} = \frac{L_{m1}}{L_s}\Psi_{qs} + \frac{L_{m1}}{L_r}\Psi_{qr} \quad .....(17)$$

$$\Psi_{dm} = \frac{L_{m1}}{L_s}\Psi_{ds} + \frac{L_{m1}}{L_r}\Psi_{dr} \quad .....(18)$$

Where:

$$L_{m1} = \frac{1}{(\frac{1}{L_m} + \frac{1}{L_s} + \frac{1}{L_r})} \quad ....(19)$$

From the previous equations the dynamic model of an induction motor is simulated as shown in figure (5).

3. A.C Drive Control Strategies

There are many types of control strategies, were built and employed according to the desired performance level. The most popular used strategies are [1, 2]:

3.1 Scalar Control

It's the simplest control method, easy to implement, and have been widely used in industry. As the name indicates, is due to the magnitude variation of the control variables only, and disregards the coupling effect of the machine.

3.2 Direct Torque Control

It's complex than scalar control, in which the errors between the reference and the estimated values of torque and flux are directly control the inverter states in order to reduce the torque and flux errors.

3.3 Adaptive Control

It is more complex than previous types, which deal with variable mechanical parameters load nature. Such controller requires adaptation or tuning of controller parameters in real time, depending on the plant parameter variation and load torque disturbance.

3.4 Vector or Field-Oriented Control

Vector or Field-Oriented Control (FOC), allows a squirrel-cage induction motor to be driven with high dynamic performance. It transforms the dynamic structure of the A.C motor into that of separately excited D.C motor [1, 2, 3]. For D.C motor, the field flux is proportional to the field current, if the field assumed to be constant and independent of armature current, the armature current provides direct control torque, so that:

$$T_e \propto I_f * I_a \quad .... (20)$$

With the induction motor transformed to d-q plane, it looks like a separately excited D.C motor. The (FOC) technique decouples the two components of stator current; one providing the air-gap flux, and the other producing the torque. These current components provide independent control of flux and torque and the characteristic is linear [1, 2, 3]. These components are transferred back to the stator frame before feeding back

to the rotor. The two components are d-axis i_{ds}^{s} analogues to field current I_f, and q-axis i_{qs}^{s} is analogues to armature current I_a of the separately excited D.C motor [1, 2]. This strategy can be implemented by align the rotor flux vector along the d-axis of the stationary frame as shown by the phasor diagram in figure (6). The fundamentals of vector control implementation can be explained in figure (7), where the motor model is presented in a synchronously rotating reference frame, the voltage-fed SPWM inverter produces three-phase voltages (v_a, v_b, v_c) according to the reference command voltages (v_a^*, v_b^*, v_c^*) the flux component of stator current ($i_{ds}^{s^*}$) and the torque component of the stator current ($i_{qs}^{s^*}$) is used as a control signals to the system, which are inversely transformed to three-phase reference currents (i_a^*, i_b^*, i_c^*), and then transferred to three-phase voltages (v_a^*, v_b^*, v_c^*) through (PI) controller [1, 2]. The vector control can be implemented by either direct or indirect method, these methods are different essentially by how the unit vector ($\cos\theta_e$ and $\sin\theta_e$) is estimated for the controller.

3.5 Sensorless Vector Control

Speed estimation is an issue of particular interest with induction motor drives where the mechanical speed of the rotor is generally different from the speed of the revolving magnetic field. The advantages of speed sensorless induction motor drives are: reduced hardware complexity, lower cost, reduced size of the drive machine, elimination of the sensor cable, better noise and electromagnetic interference immunity, increase reliability and less maintenance requirements. The operation in hostile environment mostly requires sensorless drive [3, 7].

4. Flux Vector Estimation

There are two commonly methods of flux estimation; voltage model, and current model. The first one has strong performance in high speed regions but not in low speeds. Whereas, the second method has an accepted performance in both low and high speeds [1, 4].

The current model depends on the main rotor equations in the two axes stationary frame d^s-q^s, superscript "s" referred to stationary frame quantities:

$$R_r i_{qr}^{\ s} + \frac{d\Psi_{qr}^{\ s}}{dt} - w_r \Psi_{dr}^{\ s} = 0 \quad \text{.....(21)}$$

$$R_r i_{dr}^{\ s} + \frac{d\Psi_{dr}^{\ s}}{dt} + w_r \Psi_{qr}^{\ s} = 0 \quad \text{.....(22)}$$

Adding terms $(L_m R_r/L_r)\, i_{ds}^{s}$ and $(L_m R_r/L_r)\, i_{qs}^{s}$ and simplifying, get:

$$\Psi_{qr}^{s} = \int [\frac{Lm}{Tr}\, i_{qr}^{s} + \omega_r \Psi_{dr}^{s} - \frac{\Psi_{qr}^{s}}{Tr}]. \quad (23)$$

$$\Psi_{dr}^{s} = \int [\frac{Lm}{Tr}\, i_{dr}^{s} - \omega_r \Psi_{qr}^{s} - \frac{\Psi_{dr}^{s}}{Tr}]. \quad (24)$$

Where: Tr = $\frac{Lr}{Rr}$ is the rotor time constant.

Equations (23 & 24) give rotor fluxes as a function of stator currents and speed. Therefore, knowing these signals, the rotor flux and corresponding unit vector ($\cos\theta_e$ and $\sin\theta_e$) can be estimated by means of DSP microprocessor to implement the following equations [1, 4]:

$$\begin{aligned} \overline{\Psi_r} &= \sqrt{\Psi_{qr}^{s2} + \Psi_{dr}^{s2}} \\ \Psi_{qr}^{s} &= \overline{\Psi_r}\sin\theta_e \\ \Psi_{dr}^{s} &= \overline{\Psi_r}\cos\theta_e \\ \text{Or: } \sin\theta_e &= \frac{\Psi_{qr}^{s}}{\overline{\Psi_r}} \end{aligned} \quad (25)$$

$$\cos\theta_e = \frac{\psi^s_{dr}}{\overline{\psi_r}}$$

Flux estimation by the current model requires a speed encoder, but the advantage is that the drive operation can be extended down to low and zero speed. It's important to mention, that the input signals to the estimator (i^s_{qs} and i^s_{ds}) must be filtered by a low pass filter stage. The simulation of the current model estimator can be shown in figure (8).

5. DSP Vector Control with Speed Sensor Simulation

As mentioned before, equations (25) implemented by means of DSP microprocessor to estimate the rotor flux $\overline{\Psi_r}$ and the unit vector ($\cos\theta_e$ and $\sin\theta_e$). Then two reference commands are obtained; first the torque command i^*_{qs}, and second the flux command i^*_{ds}, which are D.C values in synchronously rotating frame [1, 2, and 4]. These two setting commands are compared with the actual currents i^s_{qs} and i^s_{ds}, the error signals of the two components are converted to voltage reference signals v^*_{qs} and v^*_{ds} by means of two PI controllers, which are converted to three phase reference voltages (v^*_a, v^*_b, v^*_c) to drive the SPWM inverter at desired voltage and frequency. The flux command i^*_{ds} obtained from PI flux control loop for precision control of flux, and the torque command i^*_{qs} generated from the speed control loop. The overall close loop simulation of DSP-estimator with PI-controller field oriented speed control is illustrated in figure (9). The flux command Ψ^*_r collected with the speed command ω^*_r the lockup table to program the flux during field weakening regions. The operation performance of the motor under different speed steps is shown in figure (10).

6. Rotor Speed Estimation

The estimation of the rotor speed from the stator voltage and current is normally complex and heavily dependent on machine parameters. The parameters variation problem, particularly near zero speed, imposes a challenge in the accuracy of speed estimation.

There are many estimation techniques can be classified as follows [1, 3, 7]:

1- Slip calculation.
2- Direct synthesis from state equations.
3- Model referencing adaptive system (MRAS).
4- Speed adaptive flux observer.
5- Extended Kalman filter (EKF).
6- Slot harmonics.
7- Injection of auxiliary signal on salient rotor.

The simplest estimation technique is the slip calculation method, in which technique the speed can be estimated by calculated the slip frequency ω_{sl} and then: $\omega_r = \omega_e - \omega_{sl}$ where ω_e is the stator speed (rad/sec). The ω_{sl} is calculated from the stator currents i^s_{qr} & i^s_{dr} as follows [1, 7]:

$$\omega_{sl} = \frac{(1+\sigma * S * T_r)\, L_s\, i_{qs}}{T_r\,(\psi_{ds} - \sigma\, L_s\, i_{ds})} \quad \text{.... (26)}$$

Where:

$$\sigma = 1 - \frac{L^2_m}{L_s\, L_r} \quad \text{..... (27)}$$

$$T_r = \frac{L_r}{R_r} \quad \text{… (28)}$$

And the stator speed can be calculated as follows [1, 7]:

$$\omega_e = \frac{(v^s_{qs} - i^s_{qs}R_s)\psi^s_{ds} - (v^s_{ds} - i^s_{ds}R_s)\psi^s_{qs}}{\psi^2_s} \quad \text{….(29)}$$

By substituting equations 26 & 29 and simplified, the rotor speed ω_r can be

estimated directly. This method called "direct synthesis" and the final form of speed estimator is as follows:

$$\omega_r = \frac{1}{\overline{\psi_r^s}}\left[\begin{array}{r}(\psi_{dr}^s \dot{\psi}_{qr}^s - \psi_{qr}^s \dot{\psi}_{dr}^s) - \frac{L_m}{T_r} \\ (\psi_{dr}^s i_{qs}^s - \psi_{qr}^s i_{ds}^s)\end{array}\right] \quad \ldots\ldots(30)$$

Then by simulated this equation the estimated rotor speed can be achieved as shown in figure (11).

And the operating performance of the motor under different speed steps of the sensorless vector control DSP estimator is shown in figure (12).

7. Artificial Neural Networks

Nowadays, we have seen extensive researches and developments effort to use the intelligent system in many industrial applications, because of its strong features like: learning ability, massive parallelism, fast adaptation, inherent approximation capability, and high degree of tolerance [8, 9]. Neural Network Controller (NNC) was effectively introduced to improve the performance of nonlinear system, which are a powerful tools used to predict the optimum performance for both identification and control system. The universal approximation capabilities of multi-layer perceptron make it popular choice for modeling nonlinear systems and for implementing general-purpose controllers. The neural network is an intelligent system which could be learned or trained using an actual existing input and output table, learning or training can be achieved in real-time or off-time operation [1, 9].

Thus, these features can be employed in this work to estimate the amount of the rotor flux vector $\overline{\Psi_r}$, the unit vector ($\cos\theta_g$ and $\sin\theta_g$) and the rotor speed ω_r instead of using DSP microprocessor, which reduce the complexity of the hardware, and reduce the Electro Magnetic Interference EMI in the microprocessor performance. Also, a neural-based PI controller can be implemented instead of hardware PI controller.

7.1 Design of Neural Network Estimator

A neural network of four input neurons (i_{qs}^s , i_{ds}^s , Ψ_{qr}^s , Ψ_{dr}^s) and four output neurons ($\cos\theta_g$, $\sin\theta_g$, T_e , Ψ_r) with 20 hidden layers was trained to achieve the desired output of the estimator. It's important to mention here, that is, traditionally a large number of input and output data of different speed conditions are used to training the neural network, but in this work a single unit step signal with rise and fall-edge is used to training the neural network, which gives an excellent performance in different speed conditions. The accuracy performance of the neural network can be shown in figure (13). And the neural network estimator simulation is shown in figure (14).

By the same manner, a neural network of six input neurons (i_{qs}^s , i_{ds}^s , v_{qs}^s , v_{ds}^s, i_{qs}^s , i_{ds}^s) and one output neuron (ω_r) with 10 hidden layers was trained to achieve the desired output of the estimator. Also, the training process was done by single unit step signal with rise and fall-edge. The final neural network of the speed estimator can be shown in figure (15). And the accuracy performance of this neural-based estimator is illustrated in figure (16).

7.2 Design of Neural-based PI Controller

A single neural network has two inputs and outputs neurons with four hidden layers are used to achieve the desired control signal in both of torque and flux component PI controllers. Also, as in the neural estimator, the training process was done by using a

single unit step signal with rise and fall-edge. The simulation of the neural-based PI controller is shown in figure (17).

The overall simulation of sensorless vector control system based on neural estimator and controller is shown in figure (18). The motor performance for different speed steps is shown in figure (19), and the rotor speed accuracy performance for gradually increasing of command speed from 0-140% of rated speed with estimated unit vector are shown in figure (20).

8. **Discussion** Figure (21) illustrated performances of the three represented methods in this paper: DSP-estimator PI-controller with speed sensor, sensorless DSP-estimator PI-controller, and sensorless neural estimator and controller. From which, the obtained conclusion can be summarized as following:

1. Obviously, according to high performance demand, the three represented methods are very good solution, where the vector control gives strong performance in different speed steps, under full-load condition in both constant torque and field weakening operation regions.
2. The conventional DSP-estimator PI-controller with speed sensor gives a very good performance, in which the rise time to achieve the command speed is approximately 0.36 sec, the overshot response is less than 2%, settling time about 0.4 sec and the steady state error is less than 0.5%.
3. The sensorless DSP-estimator PI-controller gives a slower performance from the previous method, because of the time delay of the estimator low-pass filters. In which the rise time is about 0.53 sec, the overshot response is less than 5%, settling time about 0.65 sec and the steady state error is less than 0.5%.
4. The implementation of Neural estimator and controller improves the system performance of the sensorless vector control, which gives an excellent response: rise time 0.33 sec, overshot less than 1%, settling time 0.34 sec, and steady state error less than 0.2%.
5. The neural-based estimation of the unit vector, electromagnetic torque, and rotor speed are very accordant to the desired and actual values as illustrated in figure (13, 16, & 20).

9. Conclusions

The proposed method in this paper gives an excellent and superior performance of speed control of three phase induction motor, with respect to traditional DSP vector control.

The proposed method reduces the hardware complexity, and reduces the electromagnetic interference, which lead to improve the performance.

The proposed method is low pass filter needless, which reduces process time delay causing by the low pass filter.

Therefore, this method represents many features and advantages rather than conventional method.

References

[1]Bimal K. Bose, *"Modern Power Electronic and AC Drives"*, Prentice Hall, 2002.

[2] Qusay L. Hamdi, *"Design of Indirect Field-Oriented PWM Inverter for Three-Phase Induction Motor"*, Ph.D. Thesis, Al-Rasheed collage of engineering, University of Technology, 2007.

[3]Joachim Holtz, *"Sensorless Control of Induction Motor Drive"*, IEEE, Vol. 90, No. 8, Aug. 2002.

[4]Yushaizad Yusof, Abdul Halim Mohd, "*Simulation and Modeling of Stator Flux Estimator for Induction Motor Using Artificial Neural Network Technique*", IEEE, 2003.

[5]S.K. Pillai, *"A First Course on Electrical Drives"*, second edition, 1989.

[6]Fadhil A. Hassan, "*Modeling and Implementation of SVPWM Driver of 3-Phase Induction Motor*", Ms.c. thesis, University of Technology, Iraq, 2008.

[7]S. Meziane, R. Toufouti, H. Benalla, *"MRAS based Speed Control of Sensorless Induction Motor Drives"*, ICST-ACSE Journal, Vol. 7, Issue 1, 2007.

[8]Faa-Jeng Lin, Wen-Jyi Huang and Rong-Long Wai,*"A Supervisory Fazzy Neural Network Control System for Tracking Periodic Inputs"*, IEEE, Vol 7, February 1999.

[9]Wang Dazhi, Wang Zhenlei, Gu Shusheng, "*Identification and Control of Induction Motor Using Artificial Neural Network*", IEEE, Page: 751-754, 2005, chine.

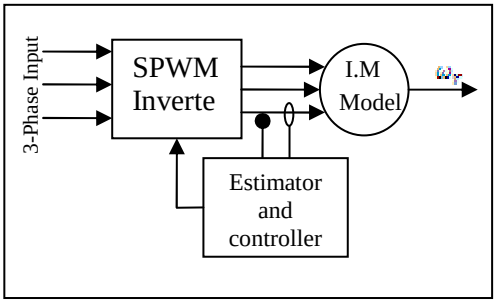

Figure (1) ***Block Diagram***

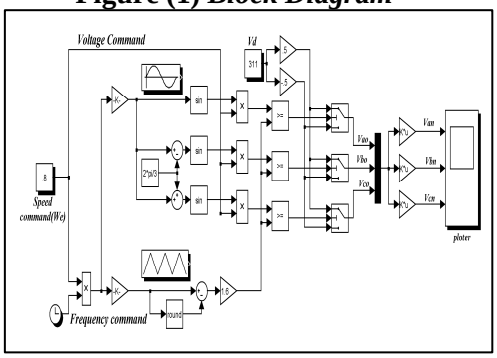

Figure (2) SPWM Simulation

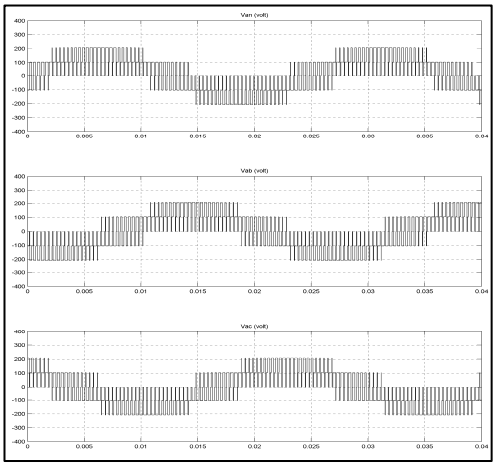

Figure (3) ***Linear Region Output Phase Voltage***

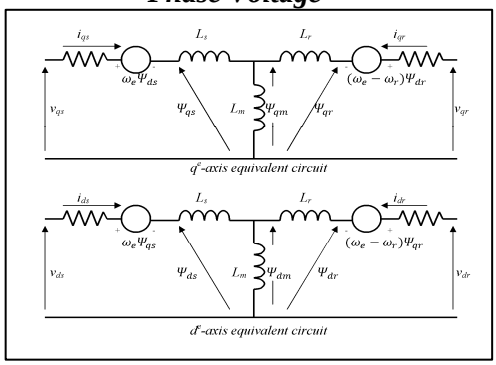

Figure (4) ***d^e-q^e I.M Equivalent Circuit***

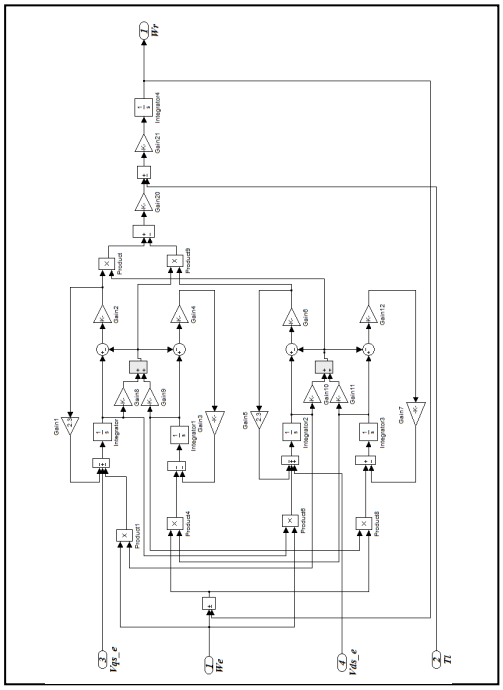

Figure (5) ***I.M Simulation***

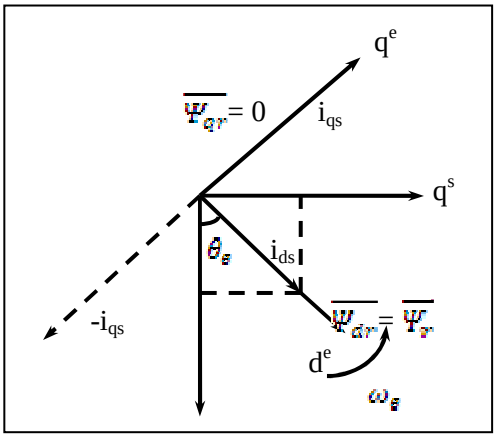

Figure (6) ***Correct Rotor Flux Orientation***

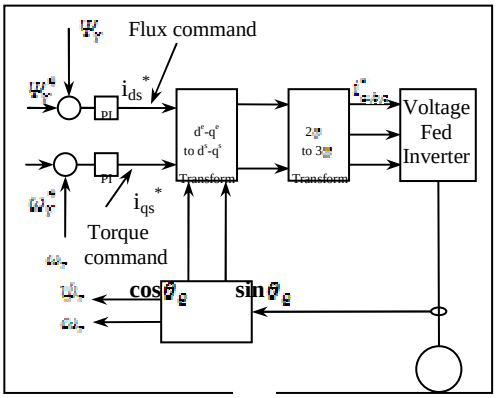

Figure (7) ***Vector Control Block Diagram***

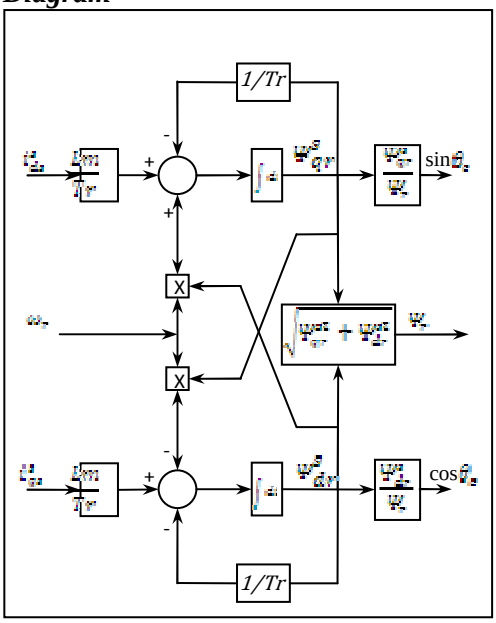

Figure (8) ***Current Model Flux Estimation***

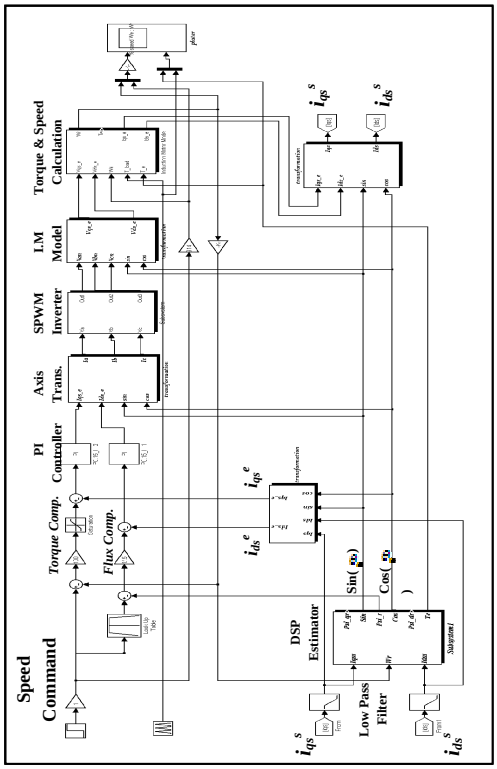

Figure (9) ***DSP-Estimator PI-Controller Overall Simulation*** **with speed sensor**

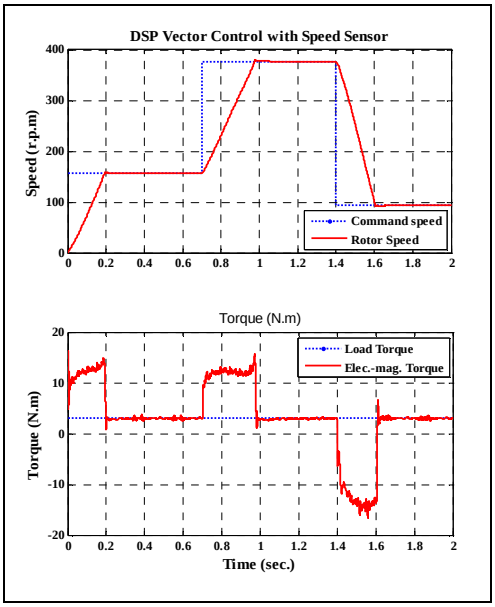

Figure (10) ***DSP-Estimator PI-Controller Performance with Speed Sensor***

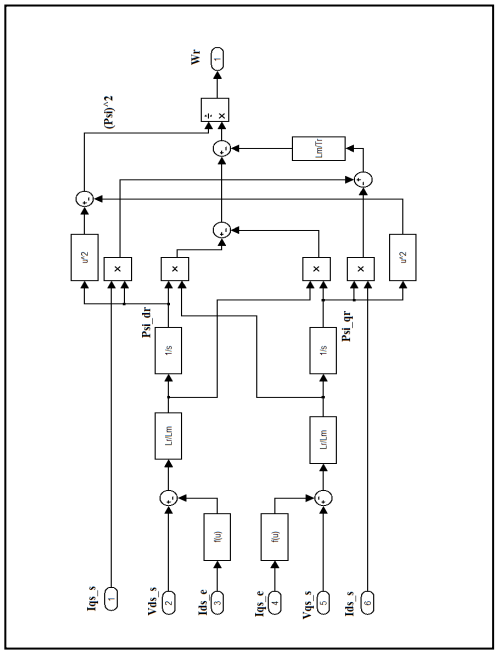

Figure (11) ***Speed Estimator Simulation***

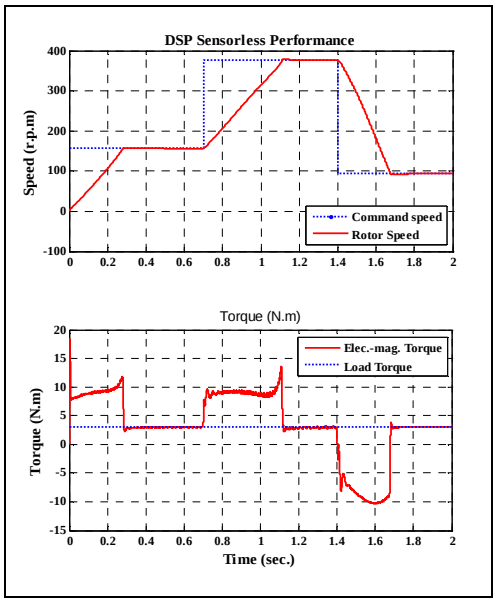

Figure (12) ***Sensorless DSP-Estimator PI-Controller Performance***

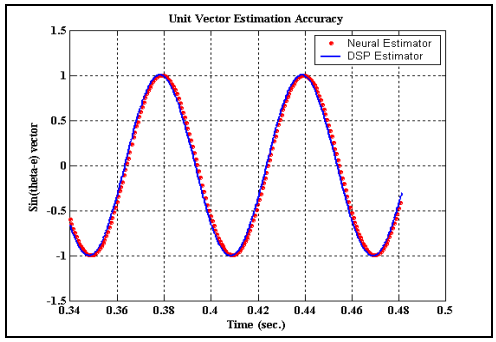

Figure (13-a) ***Unit Vector Estimation Accuracy Performance***

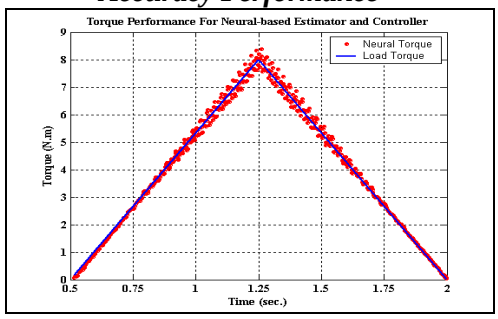

Figure (13-b) ***Torque Accuracy Performance***

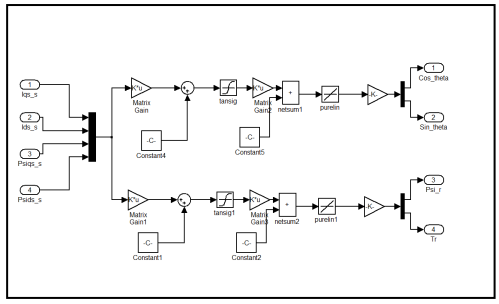

Figure (14) ***Neural Flux & Unit Vector Estimator Network Simulation***

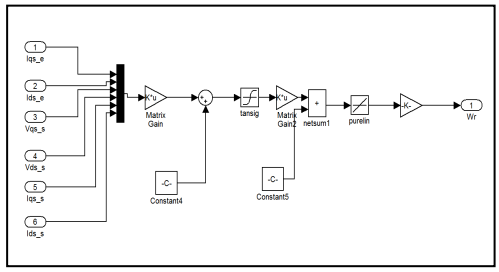

Figure (15) ***Neural Speed Estimator Network Simulation***

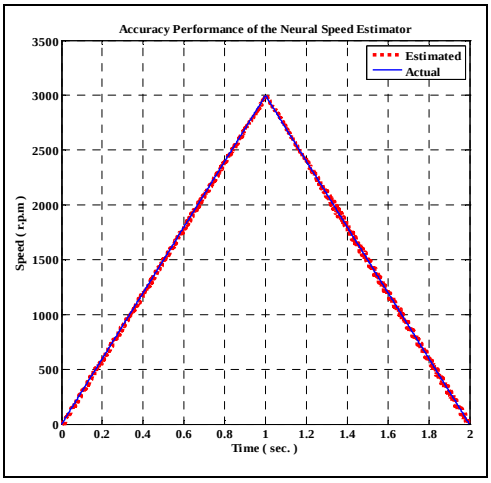

Figure (16) ***Accuracy Performance for Neural Speed Estimator***

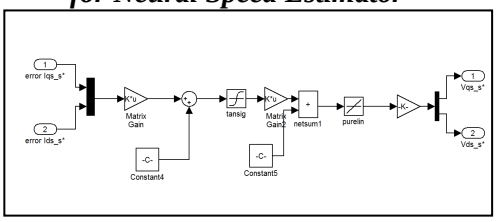

Figure (17) ***Neural-Based PI Controller Simulation***

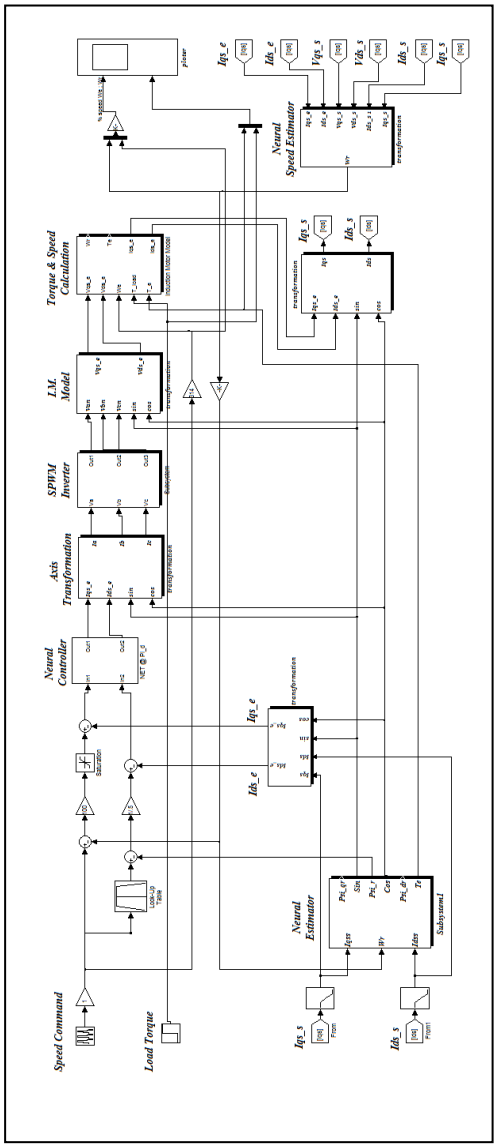

Figure (18) Overall Neural Estimator and Controller System Simulation

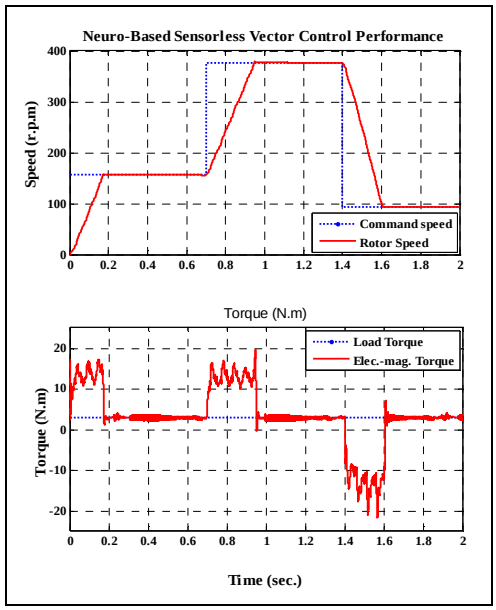

Figure (19) Sensorless Neural-Estimator and Controller Performance

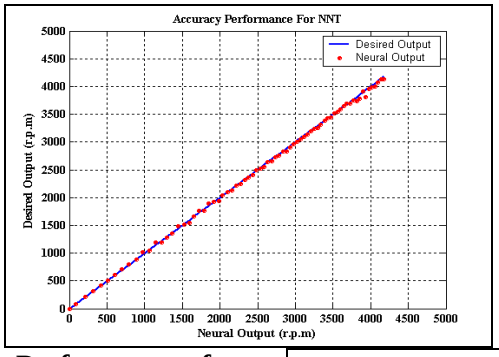

Figure (20) Accuracy Performance of the System

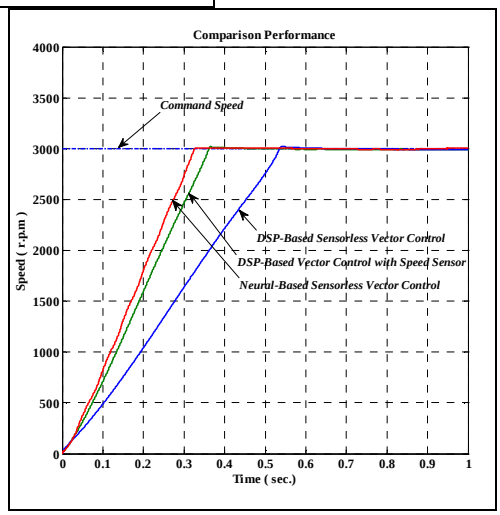

Figure (21) Comparison Performance